Plant Physiology and Biochemistry xxx (xxxx) xxx

Contents lists available at ScienceDirect

Plant Physiology and Biochemistry

journal homepage: www.elsevier.com/locate/plaphy

Transcriptome insights reveal root hair inhibition and ROS imbalance in radish seedlings treated with rhizome extracts of invasive *Fallopia* species

Katarina Šoln [a,b], Rebeka Strah [c,d], Anna Gasperl [f], Špela Baebler [c], Maruša Pompe Novak [c,e], Edith Stabentheiner [f], Maria Müller [f], Jasna Dolenc Koce [a,*]

[a] University of Ljubljana, Biotechnical Faculty, Department of Biology, Jamnikarjeva 101, SI-1000, Ljubljana, Slovenia
[b] University of Primorska, Faculty of Mathematics, Natural Sciences and Information Technologies, Department of Biodiversity, Glagoljaška 8, SI-6000, Koper, Slovenia
[c] National Institute of Biology, Večna pot 121, SI-1000, Ljubljana, Slovenia
[d] Jozef Stefan International Postgraduate School, Jamova 39, SI-1000, Ljubljana, Slovenia
[e] University of Nova Gorica, School for Viticulture and Enology, Glavni trg 8, SI-5271, Vipava, Slovenia
[f] University of Graz, Institute of Biology, Plant Sciences, NAWI Graz, Schubertstraße 51, 8010, Graz, Austria

ARTICLE INFO

Handling Editor: Shivendra Sahi

Keywords:
Allelopathy
Bohemian knotweed
Japanese knotweed
Oxidative stress
Root hair
Transcriptomics

ABSTRACT

Allelopathy is a plant-plant interaction in which an allelopathic plant negatively affects the growth of neighboring plants. Induction of oxidative stress is a common reaction to environmental stress; however, the molecular pathways between allelopathy and oxidative stress are not well understood. In this study, we analyzed the effects of 1 % and 10 % aqueous rhizome extracts of two highly invasive plants, Japanese knotweed (*Fallopia japonica*) and Bohemian knotweed (*Fallopia* × *bohemica*), on the growth, morphology, metabolome, and transcriptome of 3-day-old radish (*Raphanus sativus*) seedlings. *Fallopia* extracts decreased root biomass by up to 70 % and affected root morphology. Several genes associated with root hair formation were downregulated, resulting in decreased or completely blocked root hair development. Based on the differential gene expression, we propose a model of how *Fallopia* extracts affect radish root hair development. The extracts also induced several genes associated with the glutathione-ascorbate cycle, including glutathione peroxidases, ascorbate peroxidase, dehydroascorbate reductase, and catalase. Treated radish roots exhibited disturbed homeostasis of reactive oxygen species and oxidative stress, as indicated by the increased content of proline, total glutathione, and total cysteine, and the decreased content of total ascorbate. Both *Fallopia* extracts exhibited phytotoxic potential; however, the *F.* × *bohemica* extract caused more severe changes in radish seedlings than the *F. japonica* extract. Overall, our findings reveal that *Fallopia* extracts decrease root growth and root hair development, induce oxidative stress, and alter the expression of genes related to hormones and ROS homeostasis. As such, they provide new insights into the mechanisms underlying the invasiveness and allelopathic effects of *Fallopia*.

1. Introduction

Allelopathy is an interaction between plants in which an allelopathic plant releases secondary metabolites (allelochemicals) into its environment, suppressing the growth of nearby plants (Schandry and Becker, 2020). This phenomenon has been known for centuries and can have serious consequences for crop production (Patni et al., 2018). Moreover, allelopathy has been recognized as an additional mechanism for the dominance of many invasive plants, including knotweeds (Murrell et al., 2011). Japanese knotweed (*Fallopia japonica* var. *japonica* (Houtt.) Ronse Decr.) is listed among the 100 most invasive taxa in Europe and North America. Originally from East Asia, this perennial shrub was introduced to Europe as an ornamental plant in the 19th century (Kato-Noguchi, 2022). It then became invasive and quickly colonized new habitats, especially anthropogenically modified habitats and habitats along rivers, railways, and roads (Strgulc Krajšek and Dolenc Koce, 2015). Japanese knotweed is characterized by its rapid vegetative reproduction with underground stolons, good regenerative ability (Lawson et al., 2021), and high production of plant biomass (Frantík et al., 2013). Even more invasive is the Bohemian knotweed (*Fallopia* × *bohemica* (Chrtek and Chrtková) J. P. Bailey), a hybrid of Japanese and giant knotweed (*Fallopia sachalinensis* (F. Schmidt) Ronse Decr.). All

* Corresponding author. Department of Biology Biotechnical Faculty University of Ljubljana, Jamnikarjeva 101, SI-1000, Ljubljana, Slovenia.
E-mail address: jasna.dolenc.koce@bf.uni-lj.si (J.D. Koce).

https://doi.org/10.1016/j.plaphy.2025.110433
Received 25 April 2025; Received in revised form 19 August 2025; Accepted 23 August 2025
Available online 24 August 2025

three taxa occur in Slovenia; however, *F. japonica* and *F.* × *bohemica* are more widespread than *F. sachalinensis* and pose a serious threat to local biodiversity (Strgulc Krajšek and Dolenc Koce, 2015).

Important effects of allelopathy include suppression of seed germination and seedling growth (Schandry and Becker, 2020). Growth inhibition after exposure to *Fallopia* extracts or selected plant parts was described for white clover (*Trifolium repens*) (Mincheva et al., 2016), common nettle (*Urtica dioica*), garden cress (*Lepidium sativum*), and bush grass (*Calamagrostis epigejos*) (Moravcová et al., 2011). In our previous studies (Šoln et al., 2021, 2022, 2023), we found that extracts of *F. japonica* and *F.* × *bohemica* rhizomes inhibit seed germination and early root growth of radish (*Raphanus sativus*), which is a suitable model for studying allelopathy due to its sensitivity to various chemical compounds and rapid germination. We focused on the root because it is in contact with potentially harmful substances in soil and therefore has an important influence on seedling growth. We showed that aqueous extracts of *F. japonica* and *F.* × *bohemica* cause ultrastructural changes in radish root tips, which could explain the significantly shorter roots of exposed seedlings. The most striking ultrastructural changes were observed in root tip cells, in which electron-dense material accumulated in the endoplasmic reticulum and cytoplasm, and mitochondria were damaged (Šoln et al., 2023).

Root morphology directly affects growth, development, and nutritional status of the whole plant (Yang et al., 2012). Root hairs tie the root system to the soil substrate, facilitate water and nutrient absorption, and enable interactions with soil microbes (Zhang et al., 2023b). These tubular-shaped unicellular extensions of epidermal cells develop in the differentiation zone of a young root. Their growth and development include cell fate determination, initiation, and elongation of the hair root. According to differences in the origin and differentiation of root hairs, three types of patterns can be distinguished (Datta et al., 2011). In the type I pattern, which is characteristic of most eudicots, all epidermal cells are morphologically equivalent and can randomly differentiate into root hairs. By contrast, root hairs can develop from specialized and morphologically different epidermal cells, called trichoblasts, which are smaller and have denser cytoplasm than the surrounding hairless atrichoblasts. In the type II pattern, which is characteristic of magnoliids and some monocots, root hairs are formed after the asymmetrical cell division of meristematic epidermal cells, forming smaller trichoblasts and larger atrichoblasts, which alternate along a longitudinal cell file. In the type III pattern, which is characteristic of many families of Caryophyllales and Brassicales (including Brassicaceae with *Arabidopsis* but also *Raphanus*), root hairs also develop from trichoblasts, which are arranged in files separated by one or more files of non-hairy cells (Datta et al., 2011). Epidermal cell fate is determined by the position effect: epidermal cells in contact with two cortical cells (H-type cells) can develop into root hair cells, whereas epidermal cells in contact with only one cortical cell (N-type cells) cannot develop into root hair cells (Zhang et al., 2023b).

Each phase of root hair development is regulated by a different set of phytohormones. In the root hair determination phase, auxin, ethylene, and cytokinins act as positive regulators, whereas brassinosteroids act as negative regulators. In the root hair initiation phase, auxin, ethylene, jasmonic acid, cytokinins, and abscisic acid act as positive regulators, whereas brassinosteroids act as negative regulators. In the root hair elongation phase, auxin, ethylene, cytokinins, and jasmonic acid act as positive regulators, whereas brassinosteroids, gibberellins, and abscisic acid act as negative regulators. Phytohormones regulate root hair growth and development mainly by regulating the transcription of root hair-associated genes. To date, around 40 genes related to root hair growth and development have been identified (Lee and Cho, 2013; Vissenberg et al., 2020; Li et al., 2022).

Allelopathic stress can greatly increase the levels of reactive oxygen species (ROS) in the cells of exposed plants (Gniazdowska et al., 2015). This was also shown in our previous study, in which *Fallopia* extracts increased oxidative stress and the activity of various proteolytic enzymes in radish roots (Šoln et al., 2023). ROS are highly reactive molecules that are produced during aerobic metabolism. The best-known ROS are the superoxide radical ($O_2^{\bullet-}$), hydroxyl radical ($OH^{\bullet}$), hydrogen peroxide (H_2O_2), and singlet oxygen ($^1O_2$). ROS have a dual function in plants. At low concentrations, they act as signaling molecules and are involved in various growth and development processes (Mittler et al., 2022), such as the determination of the size of the root apical meristem (Yamada et al., 2020) and the activation of plant defenses (Hayat et al., 2016). Conversely, high ROS concentrations cause the oxidation of macromolecules, which leads to cell damage. Enzymatic and non-enzymatic antioxidants represent the most important protective mechanism against excessive ROS production, reacting with ROS and interrupting their chain reactions (Foyer and Kunert, 2024). Excessive ROS production and accumulation in plant cells overloads their antioxidant system, which prevents effective radical removal. This redox imbalance between ROS and antioxidants is known as oxidative stress. Various environmental stressors, such as high temperatures, drought (Liu et al., 2019), heavy metals (Tamás et al., 2017), and pathogenic microorganisms (Rossi et al., 2017; Lukan et al., 2020), cause ROS bursts and oxidative stress.

The molecular mechanisms of allelopathy are still not completely understood. Previous transcriptome studies of allelopathic interactions of rice and soybean with weeds (Horvath et al., 2015; Sultana et al., 2023; Zhang et al., 2019, 2023a) or plant extracts with weed-inhibiting action (Li et al., 2021) showed changes in redox-related processes, photosynthesis, secondary metabolism, and hormonal signaling. Nevertheless, only a few studies focused on linking transcriptomic changes with root growth (Zhang et al., 2022), and none of these studies investigated the effects of *Fallopia*.

In this study, we aimed to (i) analyze the effects of the aqueous extracts of *F. japonica* and *F.* × *bohemica* rhizomes on the root structure, including root hairs, of radish seedlings; (ii) determine alterations in the expression of genes associated with root hair formation and oxidative stress; and (iii) determine levels of oxidative-stress-related metabolites in radish roots.

2. Materials and methods

2.1. Preparation of Fallopia extracts

The rhizomes of *F. japonica* and *F.* × *bohemica* were collected and prepared for extraction as described in Šoln et al. (2023). Briefly, the rhizomes were rinsed, dried, lyophilized, and ground to powder. Next, 10 g of rhizome material was resuspended in 100 mL of bidistilled water, and the suspension was extracted on the orbital shaker 3020 (Gesellschaft für Labortechnik mbH, Germany) at 175 rpm and room temperature (RT) for 24 h. This suspension was filtered to prepare 10 % (w/v) aqueous extract, which was further diluted with bidistilled water to prepare 1 % extracts. Extracts were prepared fresh before each experiment.

2.2. Radish germination

Radish (*R. sativus* L.) cv. Saxa 2 seeds were placed in a Petri dish (diameter: 14 cm) on a layer of filter paper (Grade 520 A, Whatman, Maidstone, United Kingdom). To evaluate the effects of *Fallopia* on the germination and early growth of seedlings, radish seeds were watered with 10 mL of *F. japonica* or *F.* × *bohemica* extracts at two concentrations: 1 % and 10 %. Distilled water was used as a control treatment. The Petri dishes were wrapped with Parafilm, and the seedlings grew for 3 days in the growth chamber VB 0714 (Vötsch Industrietechnik, Germany) under the following conditions: 22 °C, 12 h light/12 h dark photoperiod, and 50 % humidity. For biomass determination, and glutathione and ascorbate analysis, 100 seeds were placed in one Petri dish. For proline analysis, 50 seeds were placed in one Petri dish because fresh seedlings with higher biomass are used for biochemical analysis. Five independent

replicates were performed for each treatment and each analysis. At the end of the experiment, on day 3 after exposure, roots were separated from the shoots with a scalpel. All roots from one Petri dish were pooled and weighed with an analytical scale (ScalTec, USA) to obtain fresh biomass. The average biomass of an individual seedling was calculated by dividing the pooled root biomass by the number of germinated seeds (N = 97 for control and both 1 % extracts, N = 87 for 10 % extracts).

For proline analysis, approximately 100 mg of fresh biomass was stored in 2 mL Eppendorf tubes, frozen with liquid nitrogen, and stored at −80 °C.

For glutathione and ascorbate analysis, samples were frozen with liquid nitrogen and lyophilized (VirTiS Sp Scientific Sentry 2.0, USA) for 3 days at −57.6 °C and approximately 4.5 Pa. Dry material was ground with a mortar and pestle. Samples were weighed and stored in 1.5 mL Eppendorf tubes at −20 °C.

For gene expression analyses, only radish roots treated with 10 % extracts were sampled (two 2-cm-long roots with a root tip per sample, three biological replicates per treatment). Samples were frozen with liquid nitrogen and stored in Eppendorf tubes at −80 °C.

2.3. Light and scanning electron microscopy of roots

Roots (approximately 1 cm in length, including the root tip) were fixed in 2.5 % glutaraldehyde (Roth, Germany) in Soerensen buffer (0.067 M, pH 7.0) for 3 h at room temperature (RT) and overnight at 4 °C. After washing with buffer, samples were dehydrated in a graded acetone series (high-performance liquid chromatography (HPLC) grade, Roth, Germany) and critical point dried (CO_2; CPD 030, Balzers, Lichtenstein). Dried samples were examined using a stereo microscope (Olympus SZX16, Japan; camera software: CellSensEntry, Japan), mounted on aluminum stubs using double-sided carbon impregnated tape, and sputter-coated with gold (Agar Sputter Coater, United Kingdom). An XL30 ESEM microscope (FEI, The Netherlands) in high-vacuum mode at 20 kV acceleration voltage was used to study the surface morphology of the samples. Three roots per treatment were analyzed. Images were processed with Adobe Photoshop CS5 and Adobe Illustrator CS5 software (Adobe System, USA).

2.4. RNA extraction, RNA-Seq, and differential expression analysis

Total RNA was extracted from roots with the RNeasy Plant Mini Kit (Qiagen, USA) according to the manufacturer's instructions but with an additional prewashing step (RW1) and washing step (RPE). The presence of isolated RNA was confirmed using Nanodrop (NanoDrop Technologies Inc., USA) and gel electrophoresis (Bio-Rad, USA). Next, RNA was subjected to DNase digestion (DNase I Set; Zymo Research, USA) and cleaned up using RNA Clean and Concentration kits (Zymo Research, USA). RNA concentration, integrity, and purity were assessed using Agilent BioAnalyzer 2100 and an RNA 600 Nano Kit (Agilent Technologies, USA). Library preparations for the mRNA sequencing services (HiSeq 4000, Illumina, San Diego, CA, USA) and preprocessing to remove the adapter sequences and low-quality reads were provided by Novogene (Hong Kong). The raw data (in fastq format) were analyzed and mapped to the radish reference genome (Shirasawa et al., 2020) using CLC Genomics Workbench version 12.0.3 (Qiagen, Germany) software. Data were deposited in the European Nucleotide Archive (https://www.ebi.ac.uk/ena/) under the accession number ERS12546344-ERS12546350. Principal component analysis (PCA) was performed with the same normalized data and visualized with the package ggbiplot v0.55 (Wickham, 2016). The differential expression analysis was performed using software R v4.4.1 (https://www.R-project.org/), with the DESeq2 package v1.44.0 DESeq function (Love et al., 2014). Genes with adjusted p-values of <0.05 were considered significantly differentially expressed. Genes with low counts, marked as NA for adjusted p-values in at least one of the contrasts, were filtered out. Gene set enrichment analysis (GSEA) was performed on normalized expression values obtained with edgeR v3.28.1 (Robinson et al., 2010) using a MapMan mapping file obtained by running the radish protein sequences obtained from the radish genome through Mercator software 3.6 (Lohse et al., 2014). Results are presented as TAG values, representing the percentage of genes in the gene set that positively or negatively contributed to the enrichment. Significant results were determined to be those with a false discovery rate (FDR) of ≤0.25.

2.5. Measurements of biochemical parameters associated with oxidative stress

2.5.1. Glutathione and cysteine content

The concentration of total thiols (glutathione or cysteine) and the oxidized form of thiols were measured in root samples as described by Roach et al. (2018). Approximately 12 h before the analysis, the HCl solution was prepared as follows: 20 mg of polyvinylpolypyrrolidone (Sigma, USA) was added to a 10 mL tube, which was filled with 1.1 mL of precooled 0.1 M HCl (Roth, Germany). For each sample, a separate tube was prepared and stored at 4 °C. On the next day, approximately 10 mg of dry radish root material was added into the HCl solution, homogenized with Ultra Turrax® (IKA Labortechnik, Germany) for 20 s at a speed of 24,000 rpm and centrifuged (BR4, Jouvan, France) at 4 °C and 10,000 rpm. The supernatant was then transferred to a new 2 mL Eppendorf tube.

To measure total cysteine and total glutathione, the following assay was performed. A mixture was prepared in brown 1.5 mL Eppendorf tubes consisting of 30 µL of 1 M NaOH (Merck, Germany), 280 µL of 200 mM Tricine buffer (Roth, Germany, pH 8.0), 70 µL of freshly prepared 8 mM dithiothreitol (DDT, Roth, Germany), and 280 µL of supernatant or mixed thiol standards consisting of cysteine standards (3.31, 6.63, 9.94, and 13.25 nmol/L L-cysteine, Roth, Germany) and reduced glutathione standards (32.79, 65.57, 98.36, and 131.14 nmol/L L-glutathione, Roth, Germany). The mixture was vortexed (5 s), and pH was checked with a pH meter (420 A, Orion, Finland) to adjust to 7.9–8.3. After 1 h of incubation on a Thermomixer comfort shaker (Eppendorf, Germany) at RT and 700 rpm, 100 µL of monobromobimane (Sigma, USA) was added to label the SH-groups in samples and incubated on a shaker at RT and 700 rpm. After 15 min, the reaction was stopped by adding 600 µL of 0.75 % methanesulfonic acid in water (Merck, Germany). Then the samples were centrifuged (30 min, 4 °C, 14,000 rpm), and 800 µL of supernatant was transferred to the HPLC vials.

To measure oxidized cysteine and oxidized glutathione, the following assay was performed in transparent 1.5 mL Eppendorf tubes containing 43 µL of 1 M NaOH, 400 µL of 200 mM Tricine buffer (pH 8.0), 30 µL of 50 mM N-ethylmaleimide (Sigma, USA), and 400 µL of supernatant. The mixtures were vortexed for 5 s and then incubated for 15 min on a shaker (RT, 700 rpm) protected from light. Then 500 µL of toluol (Roth, Germany) was added to the reaction mixture, vortexed for 20 s, and centrifuged for 3 min (4 °C, 14,000 rpm). The top phase with toluol was removed. This process was repeated three times. Afterwards, 500 µl of the underneath phase was transferred to a new 1.5 mL brown Eppendorf tube, and 57 µL of DTT was added. After 1 h of incubation on a shaker (RT, 700 rpm), 82 µL of monobromobimane was added and incubated on a shaker in the dark (RT, 700 rpm). After 15 min, the reaction was stopped by adding 491 µL of 0.75 % methanesulfonic acid. Samples were then centrifuged for 30 min (4 °C, 14,000 rpm), and 800 µL of supernatant was transferred to the HPLC vials.

Total thiol and oxidized forms of thiols were separated by reverse-phase HPLC with a Knauer Eurosphere II 100-5-C18 column, 250 × 4 mm, 5 µm, and a Dionex Ultimate 3000 HPLC (Dionex, Sunnyvale, CA, USA) and detected with excitation and emission wavelengths of 380 nm and 480 nm, respectively, with a fluorescence detector (FP 2020, Jasco, Tokyo, Japan). Glutathione and cysteine concentrations were calculated using external standards of GSH and cysteine, which were run with the procedure for total thiols. For the mixed thiol stock solution, 80.6 mg of reduced cysteine was weighed and transferred to a 50 mL volumetric

flask, which was filled with 0.1 M HCl. Next, 40.3 mg of reduced glutathione was weighed and transferred to a 100 mL volumetric flask, 1 mL of the cysteine stock solution was added, and the flask was filled to 100 mL with 0.1 M HCl. The mixed thiol stock solution was diluted with 0.1 M HCl to achieve different concentrations of cysteine (3.31, 6.63, 9.94, and 13.25 nmol/L) and reduced glutathione (32.79, 65.57, 98.36, and 131.14 nmol/L).

Oxidized forms of glutathione (GSSG) and cysteine were calculated by subtracting the concentration of the oxidized subsample, divided by 2, from the concentration of total glutathione or total cysteine, respectively. The calculation considers that 1 mol of oxidized thiol yields 2 mol of reduced thiol during reduction via DTT. The amount of oxidized glutathione or cysteine was subsequently expressed as percentage of the total.

2.5.2. Ascorbate content

Total ascorbate and the oxidized form of ascorbate were measured in root samples as described by Teuschler et al. (2021). The homogenization solution was prepared at least 12 h before the analysis as follows: 15–20 mg of polyvinylpolypyrrolidone (Sigma, USA) was added to a 2 mL Eppendorf tube, which was filled with 1.4 mL of 1.5 % meta-phosphoric acid (Roth, Germany). For each sample, a separate tube was prepared and stored at 4 °C. On the next day, approximately 10 mg of dry root sample was added to the homogenization solution, homogenized with Ultra Turrax® Heidolph DIAX 600 (IKA Labortechnik, Germany) for 20 s at 24,000 rpm and centrifuged (BR4, Jouvan, France) at 4 °C and 14,000 rpm. Supernatant was transferred to a new 2 mL Eppendorf tube.

To measure reduced ascorbic acid, the following assay was performed. A mixture was prepared in 1.5 mL transparent Eppendorf tubes consisting of 337.5 μL of 0.2 M Tris buffer (0.9005 g of Tricine (>99 %, Honeywell Fluka™, USA) and 25 mL of bidistilled water), 10.6 mg of EDTA Titriplex III (Merck, Germany, pH 8.0), 37.5 μL of bidistilled water, 75 μL of ortho-phosphoric acid (1:10, 85 %, Roth, Germany), and 450 μL of supernatant. To measure total ascorbic acid, the following assay was performed in 1.5 mL transparent Eppendorf tubes containing 337.5 μL of 0.2 M Tris buffer, 37.5 μL of DTT (60 mg dissolved in 1.5 mL of bidistilled water), and 450 μL of supernatant. After vortexing for 3 s, the mixture was incubated at RT on a Thermomixer comfort shaker (Eppendorf, Germany) for 10 min at 700 rpm, and then 100 μL of ortho-phosphoric acid (1:10, 85 %) was added. Both reaction mixtures were vortexed for 3 s and centrifuged for 30 min (4 °C, 14,000 rpm), and then 750 μL of supernatant was transferred to the HPLC vials.

Samples were analyzed by HPLC with a Eurosphere II 100-5-NH2 column, 250 × 4 mm (Knauer, Germany) and a Dionex Ultimate 3000 HPLC with diode array detector (Dionex, Sunnyvale, CA, USA) and detected at 250 nm.

Sample concentrations were calculated using external standards. For the ascorbate stock solution, 60.1 mg of L-ascorbic acid (Roth, Germany) was dissolved in a 20 mL volumetric flask with meta-phosphoric acid (1.5 % (w/v) in water, (Roth, Germany) and filled up to the mark. Dilutions with final concentrations of 37.56, 75.13, and 150.25 μmol/mL were prepared using meta-phosphoric acid.

2.5.3. Proline content

Proline was analyzed according to Bates et al. (1973). For free proline detection, 100 mg of fresh radish roots and 1.5 mL of 3 % sulfosalicylic acid (Merck, Germany) were added to a 2 mL Eppendorf tube. Samples were homogenized with Ultra Turrax® Heidolph DIAX 600 (IKA Labortechnik, Germany) for 20–30 s and centrifuged for 15 min (RT, 14,000 rpm). The reaction was performed in a glass eprouvette containing the following: 500 μL of ninhydrin (2.5 g ninhydrin (Roth, Germany), dissolved in 60 mL of acetic acid (100 % p. a., Roth, Germany), 40 mL of 6 M ortho-phosphoric acid (85 %, Merck, Germany), 500 μL of acetic acid (Fluka, Germany), and 500 μL of supernatant or proline standards. Proline stock solution (1 mg/mL) contained 10 mg of L-proline (Merck, Germany) in 10 mL of 3 % sulfosalicylic acid; this was then diluted with 3 % sulfosalicylic acid to obtain the following concentrations: 0, 5, 10, 15, 20, 30, and 40 μg/μL. The proline reaction mixture was incubated for 1 h at 100 °C in water bath (Waterbath B-480, Büchi, Switzerland), during which the color of the solution changed from colorless to bright red. The reaction was stopped on ice, and after approximately 10 min, toluol (Roth, Germany) was added. Samples were vortexed for 15–20 s. The upper toluol red phase was transferred to a glass cuvette (Hellma, Germany), and the absorbance was measured at 520 nm with a spectrophotometer (U-300, Hitachi, Japan).

2.6. Statistical analysis

Means and standard errors were calculated for each measured morphological and biochemical parameter. The means were compared between treatments using one-way ANOVA, and Tukey's multiple comparisons post-test was used when the differences were statistically significant. The level of significance was set at $p < 0.05$. Data were analyzed using GraphPad Prism 9.2.0 (GraphPad Software Inc., La Jolla, CA, USA).

3. Results

3.1. Fallopia extracts affect radish root morphology

The extracts of *Fallopia* rhizomes significantly affected the morphology and biomass of radish roots. At 10 %, the *F. japonica* and *F.* × *bohemica* extracts decreased root biomass by 57 % and 71 %, respectively, compared to control. Conversely, at 1 %, the *F. japonica* extract exerted a stimulatory effect, increasing root biomass by 59 %, whereas the *F.* × *bohemica* extract did not significantly affect root biomass (Fig. 1A).

Fallopia extracts distinctly altered radish root morphology. The roots of seedlings treated with *Fallopia* extracts (Fig. 1C–F) were shorter and thicker than the roots of control seedlings (Fig. 1B). Control seedlings had many well-developed root hairs (Figs. 1B and 2A). The roots of seedlings treated with 1 % extracts also developed root hairs, which were, however, less numerous and shorter (Fig. 1C, D, 2B, 2C) than those of the control seedlings. The roots of seedlings treated with 10 % *F. japonica* extract had only a few short root hairs (Figs. 1E and 2D), whereas the roots of seedlings treated with 10 % *F.* × *bohemica* extract did not develop root hairs (Figs. 1F and 2E).

3.2. Expression of genes associated with root hair development and ROS homeostasis changes after treatment with Fallopia extracts

To gain an understanding of the molecular events underlying the observed morphological changes, we performed a transcriptome analysis of radish roots treated with 10 % extracts of both *Fallopia* species. Analysis of the RNA-Seq data produced an average of 30,568,569 reads/sample, which were aligned to the radish reference genome. Of the 46,511 annotated genes, 22,565 showed sufficient expression for differential gene expression analysis.

PCA showed a clear separation between the treatments, with the first and second principal components explaining 34.5 % and 16.6 % of the variance, respectively (Fig. 3). Although still separate on the PCA plot, the samples treated with *F. japonica* extract clustered much closer to the control than the samples treated with *F.* × *bohemica* extract.

In radish roots treated with 10 % *F.* × *bohemica* extract, 8119 genes were significantly differentially expressed (compared to the control), of which 52 % were upregulated, and 48 % were downregulated. Additionally, 10 % *F. japonica* extract resulted in a similar pattern of gene expression, albeit to a lesser extent, with 708 genes differentially expressed. Between the treatments with extracts of the two *Fallopia* species, 5943 genes were differentially expressed (Supplementary Table S1).

A

Treatment	Root biomass (mg)	p-value
Control	4.90 ± 0.88	-
1% FJ	7.71 ± 0.32	0.007
1% FB	5.90 ± 0.62	0.647
10% FJ	2.33 ± 0.14	0.014
10% FB	1.57 ± 0.09	0.001

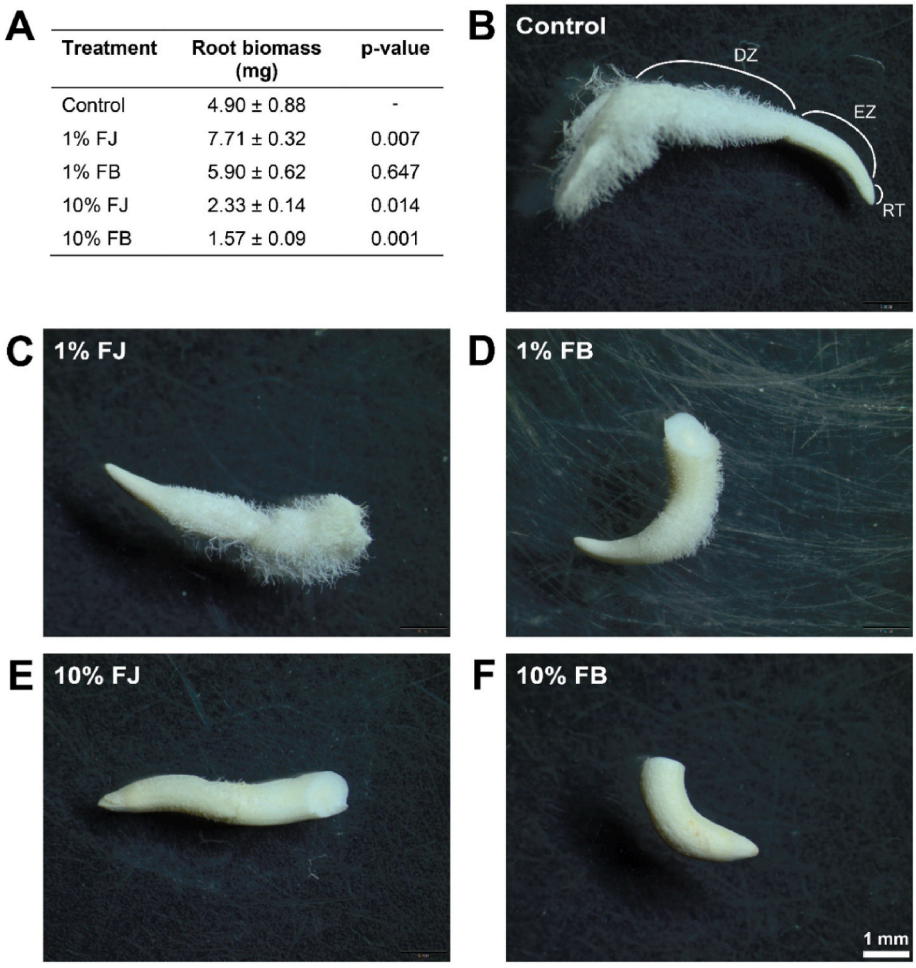

Fig. 1. Biomass and morphology of 3-day-old radish seedling roots. (A) Biomass of individual roots (mean ± SE, n = 5; p-values denote comparisons of extract vs. control treatment by ANOVA and Tukey's post-hoc test); (B–F) Stereomicroscopic images of roots treated with distilled water (Control) and 1 % and 10 % extracts of *F. japonica* (FJ) and *F.* × *bohemica* (FB) rhizomes. DZ, differentiation zone; EZ, elongation zone; RT, root tip.

At the level of biological processes, as detected by GSEA, extracts of both *Fallopia* species had similar effects on the expression of genes associated with certain metabolic and signaling pathways, including increased redox and decreased ribosomal protein metabolism, and changes in hormonal signaling (Supplementary Table S2). Regarding the hormones, we observed positive enrichment of gene sets related to abscisic acid, auxins, and jasmonate, whereas gene sets related to brassinosteroids and cytokinins remained unaffected (Table 1). The most notable difference between the *Fallopia* species was the down-regulation of chromatin structure and cell wall gene sets, and the upregulation of biotic stress gene sets, observed only after *F.* × *bohemica* treatment (Supplementary Table S1).

In the further analysis of gene expression data, we first focused on root hair development. Genes involved in the regulation of root hair growth responded to the application of *Fallopia* extracts, resulting in inhibited root hair elongation. Extracts from both *Fallopia* species caused similar changes in gene expression, although the changes induced by the *F.* × *bohemica* extract were more pronounced and resulted in a much stronger inhibition of root hair elongation, compared to *F. japonica* extract (Fig. 4, Supplementary Table S3). A component of the cell fate regulatory complex GL3/EGL3, which determines the transcription factor complex composed of WER (WEREWOLF), GL3/EGL (GLABRA 3/ENHANCER OF GLABRA 3) and TTG (TRANSPARENT TEST GLABRA), was downregulated. This complex is a positive modulator of GL2 (GLABRA 2), which is a negative regulator of root hair morphogenesis and was also downregulated after extract treatment. Furthermore, the expression of RHD6 (ROOT HAIR DEFECTIVE 6), a transcription factor that positively regulates genes involved in root hair elongation, was also downregulated, probably due to a strong upregulation of JAZ (JASMONATE-ZIM-DOMAIN PROTEIN), which inhibits EIN3 (ETHYLENE INSENSITIVE), EIL1 (EIN3-LIKE 1), and the RHD6/RSL1 (ROOT HAIR DEFECTIVE 6/RHD6-LIKE 1) complex. Consequently, RSL4 (RHD6-LIKE 4), which is involved in root hair elongation, was downregulated. Moreover, RSL2 (RHD6-LIKE 2), which is also involved in root hair elongation, was below the limit of detection. It may have been repressed by OBP4 (OBF BINDING PROTEIN 4). This gene, which blocks root hair elongation by inhibiting RSL2 transcription, was upregulated after extract treatment. Furthermore, PIN 3 and 4 (PIN-FORMED3 and 4) and DAO1 (DIOXYGENASE FOR AUXIN OXIDATION 1) were upregulated, further indicating decreased auxin levels, which can repress root hair elongation (Fig. 4). Finally, the expression of ERU (ERULUS), which is a target of ARFs (AUXIN RESPONSE FACTORS) involved in promoting root hair elongation and cell wall formation, was below the limit of detection (Fig. 4, Supplementary Table S3). By contrast, the expression of OXI1 (OXIDATIVE SIGNAL-INDUCIBLE1), involved in the regulation of root hair initiation, was not repressed by the *Fallopia* extracts (Fig. 4, Supplementary Table S3).

To assess the effects of the extracts on oxidative stress, we determined changes in the expression of genes associated with oxidative stress in our RNA-Seq dataset (Table 2, Supplementary Table 1). Both extracts upregulated the expression of several genes associated with the ascorbate-glutathione cycle, namely ascorbate peroxidase (APX3),

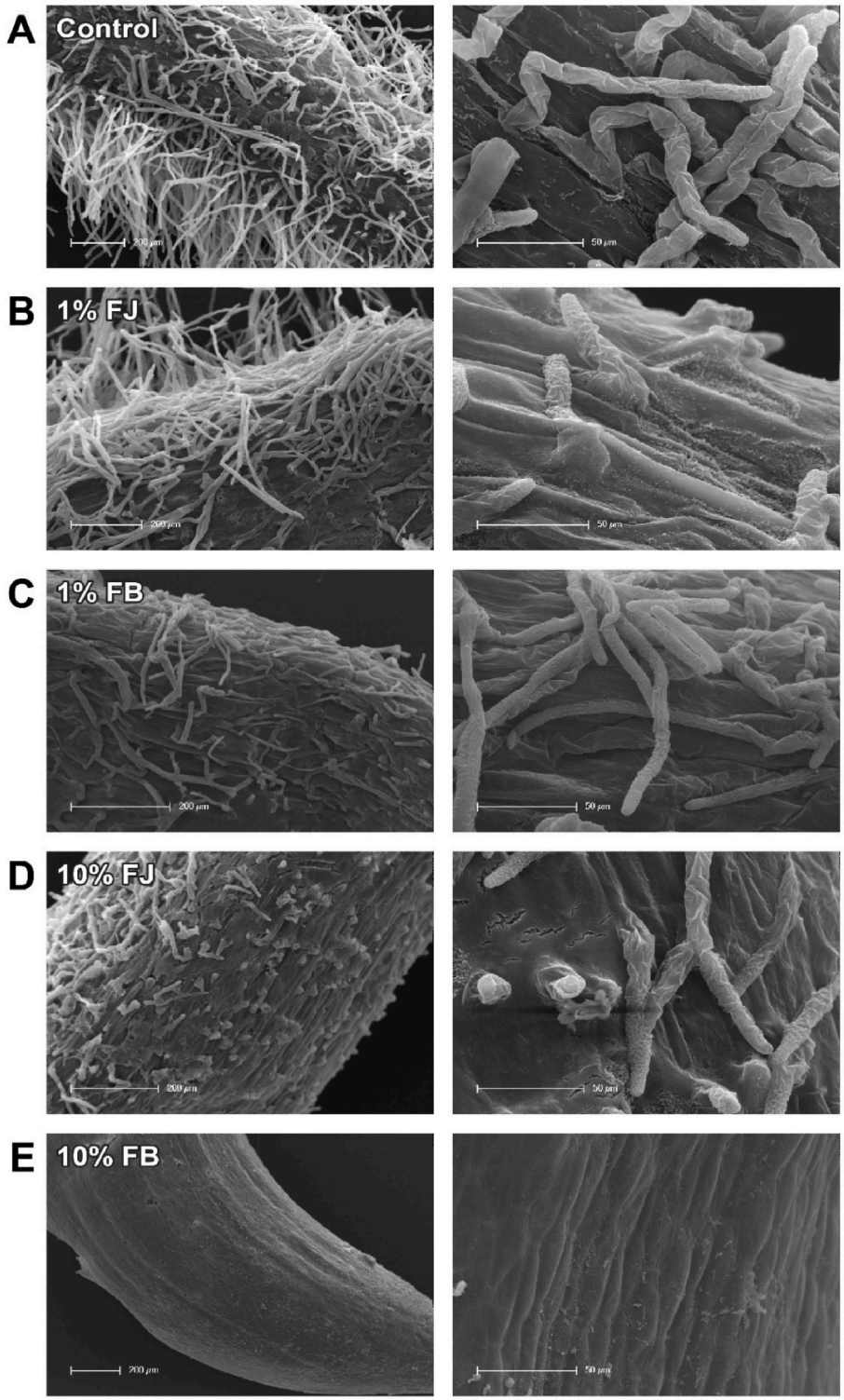

Fig. 2. Scanning electron micrographs showing root differentiation zones with visible root hairs (left, overview; right, close-up). The 3-day-old radish seedlings were treated with distilled water (Control) and 1 % and 10 % extracts of *F. japonica* (FJ) and *F.* × *bohemica* (FB) rhizomes.

dehydroascorbate reductase (DHAR), monodehydroascorbate reductase (MDAR1), glutathione reductase (GR1), several genes for glutathione peroxidase (GPX2, GPX6, GPX7), genes involved in glutathione metabolism (GSH1, GSH2), and genes for catalase (CAT2, CAT3). In all cases, the induction was stronger with the *F.* × *bohemica* extract. The response to oxidative stress was also manifested by an increased expression of respiratory burst oxidase homologues D and C (RBOHD, RBOHC), which was, however, only induced by the *F.* × *bohemica* extract.

3.3. *Fallopia extracts mainly increase the levels of oxidative stress-related metabolites in radish roots*

To complement the results observed at the gene expression level, we analyzed the levels of several metabolites associated with ROS

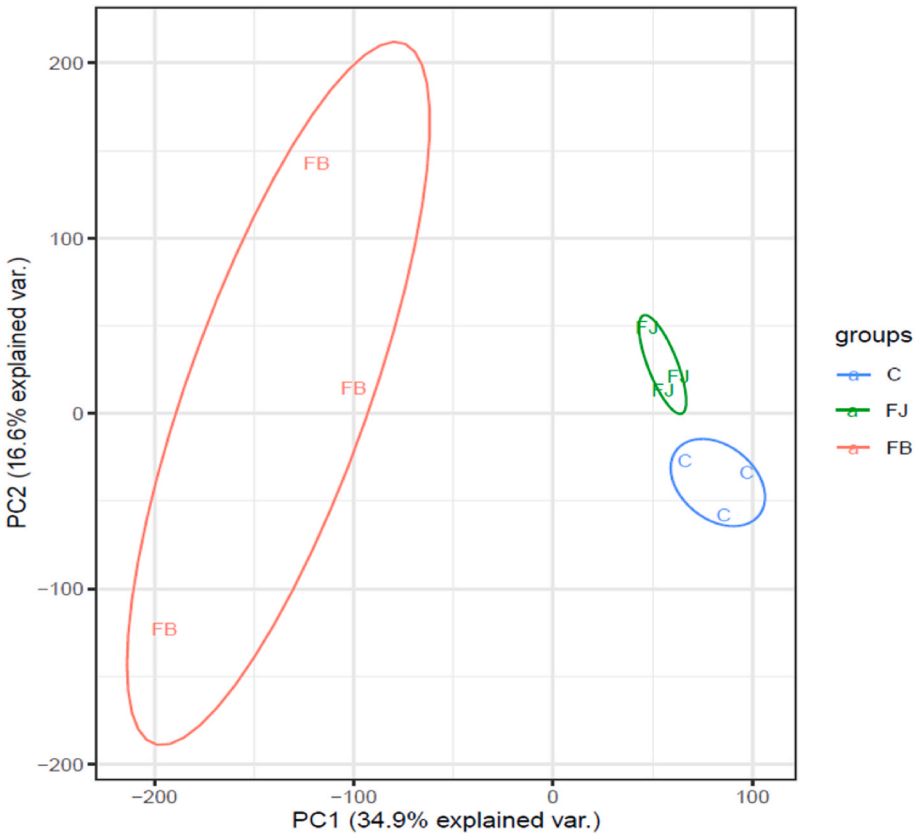

Fig. 3. Principal component analysis of the gene expression in radish roots treated with *Fallopia* extracts. C, control treatment; FB, *F.* × *bohemica* treatment; FJ, *F. japonica* treatment; PC, principal component.

Table 1
Selected results of gene set enrichment analysis for groups of hormone-related genes. For each process, the gene set name (MapMan BIN), a short description, and the number of genes contained in the BIN is listed. Statistically significant (false discovery rate-corrected Q < 0.25) differentially regulated processes between the control radish samples and samples treated with either *F.* × *bohemica* (FBvC) or *F. japonica* (FJvC) are marked with a + sign. The color intensity represents the percentage of genes contributing to process enrichment. More detailed information is provided in Supplementary Table S2.

BIN	Process	No. of genes	FBvC	FJvC
17.1	Abscisic acid metabolism	82	+	+
17.1.2	Abscisic acid signal transduction	25		+
17.1.3	Abscisic acid responsive	25	+	
17.2	Auxin metabolism	291	+	
17.2.1	Auxin synthesis and degradation	22	+	+
17.2.2	Auxin signal transduction	46		
17.2.3	Auxin responsive	221	+	
17.3	Brassinosteroid metabolism	92		
17.4	Cytokinin metabolism	62		
17.7	Jasmonate metabolism	47	+	+
17.7.1	Jasmonate synthesis and degradation	21	+	
17.7.3	Jasmonate responsive	22	+	+
17.8	Salicylic acid metabolism	19		

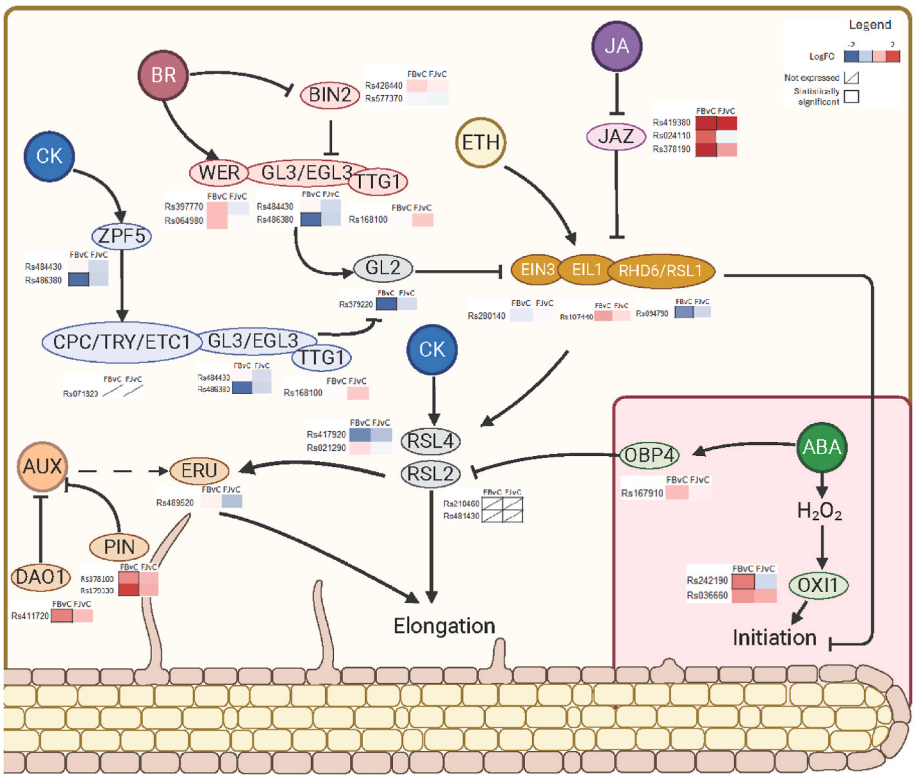

Fig. 4. The differential expression of genes involved in radish root hair development after treatment with *Fallopia* extracts. Log_2-fold changes of expression (red: upregulated, blue: downregulated) of selected genes involved in root hair initiation and elongation. The dashed line indicates omitted regulation steps. Abbreviations: C, control treatment; FB, *F.* × *bohemica* treatment; FJ, *F. japonica* treatment; JA, jasmonic acid; BR, brassinosteroids; CK, cytokinins; AUX, auxins; ABA, abscisic acid; BIN2, BRASSINOSTEROID-INSENSITIVE 2 (Rs428440, Rs577370); CPC, CAPRICE (Rs071820); DAO1, DIOXYGENASE FOR AUXIN OXIDATION 1 (Rs411720); EIL1, EIN3-LIKE1 (Rs107440); EIN3, ETHYLENE INSENSITIVE 3 (Rs280140); ERU, ERULUS (Rs489520); ETC1, ENHANCER OF TRY AND CPCs (Rs071820); GL2, GLABRA 2 (Rs379220); GL3/EGL, GLABRA 3/ENHANCER OF GLABRA 3 (Rs484430, Rs486380); JAZ8, JASMONATE-ZIM-DOMAIN PROTEIN 8 (Rs419380, Rs024110); JAZ9, JASMONATE-ZIM-DOMAIN PROTEIN 9 (Rs378190); OBP4, OBF BINDING PROTEIN 4 (Rs167910); OXI1, OXIDATIVE SIGNAL-INDUCIBLE1 (Rs242190, Rs036660); PIN3, PIN-FORMED3 (Rs378100); PIN4, PIN-FORMED4 (Rs179330); RHD6, ROOT HAIR DEFECTIVE 6 (Rs094790); RSL2, RHD6 LIKE 2 (Rs210460, Rs481430); RSL4, RHD6 LIKE 4 (Rs417920, Rs021290); TRY, TRIPTYCHON (Rs071820); TTG, TRANSPARENT TEST GLABRA (Rs168100); WER, WEREWOLF (Rs397770, Rs064980); ZFP5, ZINC FINGER PROTEIN 5 (Rs249120, Rs409650). (For interpretation of the references to color in this figure legend, the reader is referred to the Web version of this article.)

homeostasis and oxidative stress in radish seedling roots treated with *Fallopia* extracts. Total glutathione concentrations were significantly increased by the 10 % extracts of *F. japonica* and *F.* × *bohemica* but not the 1 % extracts (Fig. 5A). The concentrations of oxidized glutathione (Fig. 5B) were not affected by the extracts, except for the 1 % *F. japonica* extract. The concentrations of total cysteine (Fig. 5C) and oxidized cysteine (Fig. 5D) were significantly increased by the 10 % extracts but not the 1 % extracts. Proline concentrations (Fig. 5G) were significantly increased by the 10 % extracts but not the 1 % extracts. Conversely, the concentrations of total ascorbate (Fig. 5E) were lower by up to one third by 10 % *Fallopia* extracts, whereas 1 % extracts exerted no effects. The concentrations of oxidized ascorbate (Fig. 5F) were not significantly changed by the extracts.

4. Discussion

Allelopathy is considered one of the possible mechanisms for plant invasiveness (Murrell et al., 2011). In this study, we investigated early changes in the roots of 3-day-old radish seedlings after exposure to the aqueous rhizome extracts of invasive *F. japonica* and *F.* × *bohemica*. Transcriptome analyses revealed that 10 % extracts disrupt ROS homeostasis and induce significant oxidative stress in radish seedlings. These molecular responses are closely associated with the inhibition of root hair formation, a critical process for nutrient and water uptake in early plant development.

4.1. *Fallopia* extracts affect root mass and formation of root hairs in radish seedlings

Short-term exposure to 10 % extracts of *F. japonica* and *F.* × *bohemica* rhizomes resulted in radish roots with significantly smaller biomass and inhibited root hair development. These morphological changes were accompanied by transcriptomic alterations, particularly in genes associated with hormonal regulation, oxidative stress responses, and root hair differentiation. The more than 50 % smaller root biomass compared to the control confirms the previously described negative effects of invasive *Fallopia* on radish after 3 and 7 days of exposure (Šoln et al., 2021, 2023). The tendency towards shorter and thicker roots is related to the structure of these young roots, which have smaller cells arranged in more cell layers than control roots (Šoln et al., 2021). The cause of the altered root growth can be attributed to the chemical composition of *Fallopia* rhizomes. They contain the allelochemicals epicatechin (36 mg/g), emodin (14 mg/g), and resveratrol, with 24 % more resveratrol in *F.* × *bohemica* (26 mg/g) than in *F. japonica* (21 mg/g) rhizomes (Šoln et al., 2022). The higher content of resveratrol in *F.* × *bohemica* rhizomes is reflected in the more pronounced negative effects of this species' extract not only at the morphological but also at the molecular and biochemical levels.

The decreased expression of transcripts related to ribosome biogenesis in treated radish roots in this study indicates a decrease in protein synthesis, which is important for root cell growth. Only a few studies have aimed to decipher the molecular mechanisms of allelopathic effects

Table 2
Selected differentially expressed genes associated with oxidative stress in radish roots after 3-day exposure to 10 % extracts of *F. japonica* and *F.* × *bohemica*. Gene IDs and descriptions are shown together with the corresponding log_2-fold changes, compared to control (bold in case of statistically significant changes, $p < 0.05$; negative binomial general linear model fitting and Walsh test). Downregulated and upregulated changes are shown in blue and red, respectively.

Gene name	Gene description	*F. japonica*	*F.* × *bohemica*
Rs274120	Ascorbate peroxidase 3 (APX3)	0.31	**3.63**
Rs014260	Dehydroascorbate reductase (DHAR)	**1.11**	**2.18**
Rs414100	Dehydroascorbate reductase (DHAR)	**1.31**	**1.16**
Rs258150	Monodehydroascorbate reductase 1 (MDAR1)	**0.64**	**1.00**
Rs278980	Glutathione-disulfide reductase (GR1)	**0.52**	**0.68**
Rs130850	Glutathione peroxidase 2 (GPX2)	**1.51**	**1.66**
Rs355830	Glutathione peroxidase 2 (GPX2)	**1.16**	**1.76**
Rs587910	Glutathione peroxidase 6 (GPX6)	**1.22**	**2.01**
Rs154370	Glutathione peroxidase 7 (GPX7)	0.09	**1.13**
Rs055540	Glutamate-cysteine ligase (GSH1)	0.50	**1.23**
Rs170130	Glutathione synthetase 2 (GSH2)	0.36	**0.71**
Rs430200	Catalase 2 (CAT2)	−0.44	**1.64**
Rs414540	Catalase 3 (CAT3)	0.30	**3.3**
Rs524890	Catalase 3 (CAT3)	**1.19**	**4.42**
Rs016930	Catalase 3 (CAT3)	1.51	**4.56**
Rs172640	Respiratory burst oxidase homologue D (RBOHD)	−0.83	**2.07**
Rs132220	Respiratory burst oxidase protein C / root hair defective (RBOHC/RHD2)	0.03	**1.58**

in roots. Decreased root growth and weakened root tip activity in *Arabidopsis thaliana* exposed to extracts of the invasive weed *Conyza canadensis* were associated with the accumulation of ROS and the increased expression of ROS- and signaling-associated genes, such as genes for receptor kinases and calcium signaling, and by perturbed hormonal regulation at the transcriptome level (Zhang et al., 2022). In our study, transcripts related to abscisic and jasmonic acid were notably induced. As both serve as stress-response regulators, they likely trigger stress-induced growth reduction (Savchenko et al., 2019; Juteršek et al., 2022).

Auxin homeostasis is also important for optimal root growth. Some allelochemicals, such as weisiensin B, can influence auxin transport and increase auxin concentration in the root tip, thereby affecting root growth (Li et al., 2019). In our study, we observed changes in the expression of some genes involved in auxin metabolism and signaling in radish roots treated with *Fallopia* extracts. For example, PIN3, PIN4, and DAO1 were upregulated, suggesting perturbed auxin localization, which can inhibit root hair elongation. PIN3 and PIN4 inhibit root hair elongation by auxin efflux from root hair cells (Retzer and Weckwerth, 2021). DAO1 is the major indole-3-acetic acid oxidase and is involved in the spatiotemporal inactivation of auxin (Zhang et al., 2016).

Auxins also influence root hair formation, as increased auxin levels in epidermal cells trigger the development of root hairs and promote their proliferation (Kohli et al., 2022). Our study showed that 10 % extracts of *F. japonica* and *F.* × *bohemica* partially or completely inhibited root hair formation. Similarly, the allelochemical artemisinin decreased both the length and density of root hairs in *A. thaliana* (Yan et al., 2018), and coumarin altered root hair formation, particularly through its influence on polar auxin transport (Lupini et al., 2014). The changes in root morphology of *Fallopia*-treated radish seedlings could be related to the previously mentioned allelopathic compounds resveratrol, epicatechin, and emodin, and the more pronounced negative effects of *F.* × *bohemica* extract on root hairs could be attributed to higher resveratrol content.

Moreover, we observed a deregulation of other genes involved in root hair initiation and elongation. The GL3/EGL3-TTG complex plays a central role in determining cell fate in root epidermis, including root hairs (Song et al., 2024). When bound to WER, it induces the expression of GL2 and CPC (Lin et al., 2015). CPC competes with WER for binding to the GL3/EGL3-TTG complex, inhibiting the expression of GL2. GL2 itself is a negative regulator of root hair growth, inhibiting the formation of the complex of RHD6 and its homolog RSL1 (Tominaga-Wada et al., 2017). When this complex is present, it activates the expression of RSL2 and RSL4, which play an active role in root hair elongation (Bruex et al., 2012). In our transcriptome dataset, JAZ8 and JAZ9 were upregulated under both *Fallopia* extracts. Several JAZ proteins in *Arabidopsis* can inhibit the interaction between RHD6 and RSL1, thereby blocking the elongation of root hairs (Han et al., 2020). Whether this interaction also occurs between the RHD6/RSL1 complex and JAZ9 protein in radish remains to be confirmed. The morphologically changed smaller roots with few or even no root hairs can result in decreased water and nutrient uptake, thereby impairing seedling growth and development. This effect of *Fallopia* extracts confirms their allelopathic activity and reveals a new potential mechanism of invasiveness.

4.2. ROS homeostasis is disturbed in radish seedlings after exposure to Fallopia extracts

Transcriptomic data also revealed upregulation of genes involved in ROS detoxification, including glutathione peroxidase (GPX), glutathione reductase (GR), and ascorbate peroxidase (APX), particularly after treatment with *F.* × *bohemica* extract. These changes indicate a stress-induced activation of antioxidant defense mechanisms. However, the depletion of reduced ascorbate and increased expression of RBOHD suggest an imbalance in the ascorbate-glutathione cycle, contributing to oxidative stress.

Fallopia extracts not only alter the root morphology of radish seedlings but also increase the amount of oxidative stress markers and the activity of various proteolytic enzymes in their roots (Šoln et al., 2023). We have now further investigated the plant's defense mechanisms

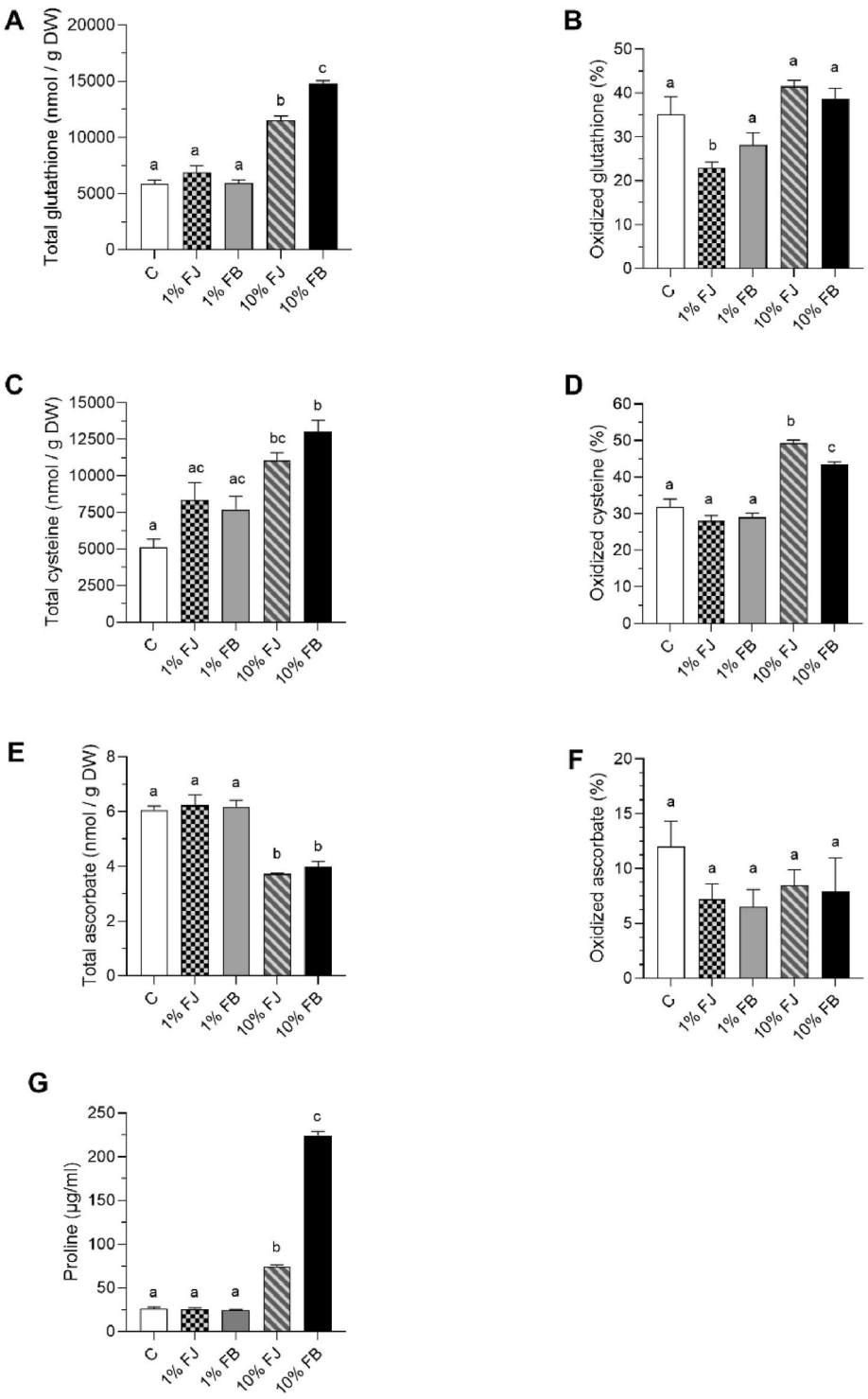

Fig. 5. The contents of antioxidants in roots of 3-day-old radish seedlings. The seedlings were treated with 1 % and 10 % extracts of *F. japonica* (FJ) and *F.* × *bohemica* (FB), and the control seedlings (C) were treated with distilled water. (A) Total glutathione; (B) oxidized glutathione; (C) total cysteine; (D) oxidized cysteine; (E) total ascorbate; (F) oxidized ascorbate; (G) free proline. Data are presented as means ± SE (n = 5). Different letters indicate statistically significant differences between treatments ($p < 0.05$; ANOVA and Tukey's post-hoc test). DW, dry weight.

against oxidative stress, highlighting the role of antioxidants. Two of the most important non-enzymatic antioxidants in plants are ascorbate and glutathione, which also act as coenzymes and are involved in post-translational modifications (Gasperl et al., 2022). In the ascorbate-glutathione cycle, these two compounds act together with specific enzymes to protect cells from oxidative damage by rapidly detoxifying H_2O_2 and maintaining ROS homeostasis (Hasanuzzaman et al., 2017; Noctor et al., 2018; Foyer and Kunert, 2024). In our study, 1 % *Fallopia* extracts did not significantly alter the content of glutathione, cysteine, or ascorbate. Proline, another prominent marker of oxidative stress (Renzetti et al., 2025), also remained at control levels. Thus, seedlings exposed to 1 % extracts could maintain ROS homeostasis and roots showed no negative effects.

Nevertheless, 10 % extracts increased oxidative stress and disrupted

ROS homeostasis, as shown by altered levels of glutathione, ascorbate, and expression of certain antioxidant enzymes. *F.* × *bohemica* extract has a 25 % higher resveratrol content than *F. japonica* extract (Šoln et al., 2022) and was thus more effective in inducing oxidative stress. The content of total glutathione increased significantly in the treated radish roots. The amount of the oxidized form, GSSG, remained largely at the control level, indicating that more of the reduced form, GSH, was present. GSH can react with ROS and reduces oxidative stress, prevents lipid peroxidation, and protects cell membranes (Hasanuzzaman et al., 2017). The expression of GPX, which converts GSH into GSSG, was upregulated, as was previously shown for juglone-treated rice (*Oryza sativa*) (Chi et al., 2011). The higher expression of GPX genes is related to a higher amount of GSH in the roots exposed to the *F.* × *bohemica* extract. Genes coding for proteins for the *de novo* synthesis of glutathione, glutamate cysteine ligase, and glutathione synthase were significantly induced by the *F.* × *bohemica* extract. Glutathione reductase, by converting GSSG to GSH, prevents the accumulation of the oxidized form in cells while providing enough reduced form to enable new reactions and neutralize radicals (Foyer and Kunert, 2024). In our study, GR1 gene expression was slightly induced, indicating that the glutathione part of the cycle continues to function effectively in radish root cells despite allelopathic stress.

Ascorbate modulates several fundamental functions in plants (Akram et al., 2017) and is an essential antioxidant and ROS scavenger that is more effective than GSH in scavenging superoxide anion radicals and singlet oxygen (Foyer and Kunert, 2024). After exposure of radish to 10 % *Fallopia* extracts, the total ascorbate content decreased significantly, whereas the level of the oxidized form remained at the control level. Dehydroascorbate reductase catalyzes the conversion of dehydroascorbate to ascorbate while oxidizing GSH to GSSG, which is regenerated to GSH by GR (Akram et al., 2017; Foyer and Kunert, 2024). In our study, we observed increased gene expression of dehydroascorbate reductase, which only partially compensates for the higher demand for reduced ascorbate.

APX reduces H_2O_2 to water using ascorbate as an electron donor (Li, 2023). In our study, *F.* × *bohemica* extract significantly increased APX3 expression in radish seedling roots. This concurs with studies that demonstrate that allelopathic stress increases the activity of H_2O_2-degrading enzymes (Mahdavikia et al., 2017). It is well known that ROS induce RBOHs that trigger ROS production (ROS wave) and cause stress-specific imbalances that alter the levels of ROS and stress-associated metabolites (Mittler et al., 2022). In our study, RBOHD expression was significantly increased by 10 % *F.* × *bohemica* extract. This upregulation of RBOHD together with the decreased levels of ascorbate by 10 % *Fallopia* extracts indicates stress-induced disturbances in ROS homeostasis, resulting in increased oxidative stress in radish root cells.

We also found increased expression of several catalase genes, especially CAT3. Another explanation for the decrease in reduced ascorbate might be that decreased ascorbate levels activate local programmed cell death (Foyer and Kunert, 2024). In our study, 10 % *Fallopia* extracts significantly increased the levels of total cysteine and oxidized cysteine in radish roots. Of note, the cysteine residue with its nucleophilic properties contributes to the high reducing potential of the glutathione molecule (Hasanuzzaman et al., 2017).

Another prominent non-enzymatic antioxidant involved in the neutralization of ROS (OH^- and $^1O_2$) is proline, an osmolyte which prevents cell damage due to lipid peroxidation. When plants are stressed, intracellular proline concentrations increase (Renzetti et al., 2025). This was observed in lettuce seedlings (*Lactuca sativa*) treated with the allelochemicals umbelliferone and daphnoretin (Yan et al., 2016), in radish seedlings treated with *Mentha* × *piperita* extracts (Mahdavikia et al., 2017), and in radish seedlings treated with 10 % *Fallopia* extracts in this study. High proline content is consistent with the absence of lipid peroxidation previously observed in 3-day-old radish seedlings after exposure to *Fallopia* extracts (Šoln et al., 2023).

5. Conclusion

This study demonstrates that allelopathic stress induced by rhizome extracts of invasive *F. japonica* and *F.* × *bohemica* negatively affects root development in radish seedlings by disrupting ROS homeostasis and inducing oxidative stress. Transcriptome analyses revealed significant changes in the expression of genes involved in antioxidant defense and root hair development. The inhibition of root hair formation, particularly by *F.* × *bohemica* extract, is likely mediated by altered hormonal signaling and increased oxidative stress. These findings provide insights into the allelopathic effects of invasive knotweeds and their potential role in plant invasiveness. The results of differential expression of genes complement the current knowledge on the regulation of root hair formation and a model of gene regulation causing defective root hair development is proposed.

CRediT authorship contribution statement

Katarina Šoln: Writing – review & editing, Writing – original draft, Visualization, Resources, Methodology, Investigation, Formal analysis, Conceptualization. **Rebeka Strah:** Writing – review & editing, Visualization, Resources, Methodology, Investigation, Formal analysis, Data curation. **Anna Gasperl:** Writing – review & editing, Supervision, Resources, Methodology. **Špela Baebler:** Writing – review & editing, Visualization, Supervision, Resources, Methodology, Investigation, Funding acquisition, Conceptualization. **Maruša Pompe Novak:** Writing – review & editing, Supervision, Resources, Methodology, Investigation, Funding acquisition, Formal analysis, Conceptualization. **Edith Stabentheiner:** Writing – review & editing, Supervision, Resources, Methodology. **Maria Müller:** Writing – review & editing, Resources, Methodology. **Jasna Dolenc Koce:** Writing – review & editing, Writing – original draft, Visualization, Supervision, Resources, Project administration, Methodology, Funding acquisition, Conceptualization.

Funding information

This work was financially supported by the Slovenian Research and Innovation Agency (grant numbers P1-0212 and P4-0165).

Declaration of competing interest

The authors declare that they have no known competing financial interests or personal relationships that could have appeared to influence the work reported in this paper.

Acknowledgements

The authors are grateful to Dr. Aleš Kladnik for help with image analysis and image editing, Dr. Maks Merela and his co-workers for rhizome grinding, Regina Willfurth and Klaus Remele for help with biochemical analysis, and Teja Grubar for help with RNA isolation. In addition, K. Šoln would like to thank the World Federation of Scientists for a one-year postdoctoral research fellowship 2023/2024. We also thank Dr. Eva Veronica Lasic for editing and reviewing a draft of this manuscript.

Appendix A. Supplementary data

Supplementary data to this article can be found online at https://doi.org/10.1016/j.plaphy.2025.110433.

Data availability

Data will be made available on request.

References

Akram, N.A., Shafiq, F., Ashraf, M., 2017. Ascorbic acid – a potential oxidant scavenger and its role in plant development and abiotic stress tolerance. Front. Plant Sci. 8, 613. https://doi.org/10.3389/fpls.2017.00613.

Bates, L.S., Waldren, R.P., Teare, I.D., 1973. Rapid determination of free proline for water-stress studies. Plant Soil 39, 205–207. https://doi.org/10.1007/BF00018060.

Bruex, A., Kainkaryam, R.M., Wieckowski, Y., Kang, Y.H., Bernhardt, C., Xia, Y., Zheng, X., Wang, J.Y., Lee, M.M., Benfey, P., Woolf, P.J., Schiefelbein, J., 2012. A gene regulatory network for root epidermis cell differentiation in arabidopsis. PLoS Genet. 8 (1), e1002446. https://doi.org/10.1371/journal.pgen.1002446.

Chi, W.C., Fu, S.F., Huang, T.L., Chen, Y.A., Chen, C.C., Huang, H.J., 2011. Identification of transcriptome profiles and signalling pathways for the allelochemical juglone in rice roots. Plant Mol. Biol. 77 (6), 591–607. https://doi.org/10.1007/s11103-011-9841-6.

Datta, S., Kim, C.M., Pernas, M., Pires, N.D., Proust, H., Tam, T., Vijayakumar, P., Dolan, L., 2011. Root hairs: development, growth and evolution at the plant-soil interface. Plant Soil 346, 1–14. https://doi.org/10.1007/s11104-011-0845-4.

Foyer, C.H., Kunert, K., 2024. The ascorbate-glutathione cycle coming of age. J. Exp. Bot. 75 (9), 2682–2699. https://doi.org/10.1093/jxb/erae023.

Frantík, T., Kovářová, M., Koblihová, H., Bartůňková, K., Nývltová, Z., Vosátka, M., 2013. Production of medically valuable stilbenes and emodin in knotweed. Ind. Crop. Prod. 50, 237–243. https://doi.org/10.1016/j.indcrop.2013.07.017.

Gasperl, A., Zellnig, G., Kocsy, G., Müller, M., 2022. Organelle specific localisation of glutathione in arabidopsis grown under different light intensities and spectra. Histochem. Cell Biol. 158 (3), 213–227. https://doi.org/10.1007/s00418-022-02103-2.

Gniazdowska, A., Krasuska, U., Andrzejczak, O., Soltys, D., 2015. Allelopathic compounds as oxidative stress agents: yes or no. In: Gupta, A.U., Igamberdiev, K.J. (Eds.), Reactive Oxygen and Nitrogen Species Signaling and Communication in Plants. Springer International Publishing, Switzerland, pp. 155–176. https://doi.org/10.1007/978-3-319-10079-1.

Han, X., Zhang, M., Yang, M., Hu, Y., 2020. Arabidopsis JAZ proteins interact with and suppress RHD6 transcription factor to regulate jasmonate-stimulated root hair development. Plant Cell 32 (4), 1049–1062. https://doi.org/10.1105/tpc.19.00617.

Hasanuzzaman, M., Nahar, K., Anee, T.I., Fujita, M., 2017. Glutathione in plants: biosynthesis and physiological role in environmental stress tolerance. Physiol. Mol. Biol. Plants 23 (2), 249–268. https://doi.org/10.1007/s12298-017-0422-2.

Hayat, S., Cheng, Z., Ahmad, H., Ali, M., Chen, X., Wang, M., 2016. Garlic, from remedy to stimulant: evaluation of antifungal potential reveals diversity in phytoalexin allicin content among garlic cultivars; allicin containing aqueous garlic extracts trigger antioxidants in cucumber. Front. Plant Sci. 7, 1–15. https://doi.org/10.3389/fpls.2016.01235.

Horvath, D.P., Hansen, S.A., Moriles-Miller, J.P., Pierik, R., Yan, C., Clay, D.E., Scheffler, B., Clay, S.A., 2015. RNAseq reveals weed-induced PIF3-like as a candidate target to manipulate weed stress response in soybean. New Phytol. 207 (1), 196–210. https://doi.org/10.1111/nph.13351.

Juteršek, M., Petek, M., Ramšak, Ž., Moreno-Giménez, E., Gianoglio, S., Mateos-Fernández, R., Orzáez, D., Gruden, K., Baebler, Š., 2022. Transcriptional deregulation of stress-growth balance in *Nicotiana benthamiana* biofactories producing insect sex pheromones. Front. Plant Sci. 13, 941338. https://doi.org/10.3389/fpls.2022.941338.

Kato-Noguchi, H., 2022. Allelopathy of knotweeds as invasive plants. Plants 11 (1:3). https://doi.org/10.3390/plants11010003.

Kohli, P.S., Maurya, K., Thakur, J.K., Bhosale, R., Giri, J., 2022. Significance of root hairs in developing stress-resilient plants for sustainable crop production. Plant Cell Environ. 45 (3), 677–694. https://doi.org/10.1111/pce.14237.

Lawson, J.W., Fennell, M., Smith, M.W., Bacon, K.L., 2021. Regeneration and growth in crowns and rhizome fragments of Japanese knotweed (*Reynoutria japonica*) and desiccation as a potential control strategy. PeerJ 9, e11783. https://doi.org/10.7717/peerj.11783.

Lee, R.D.-W., Cho, H.-T., 2013. Auxin, the organizer of the hormonal/environmental signals for root hair growth. Front. Plant Sci. 4, 448. https://doi.org/10.3389/fpls.2013.00448.

Li, S., 2023. Novel insights into functions of ascorbate peroxidase in higher plants: more than a simple antioxidant enzyme. Redox Biol. 64, 102789. https://doi.org/10.1016/J.redox.2023.102789.

Li, P., Ding, L., Zhang, L., He, J., Huan, Z., 2019. Weisiensin B inhibits primary and lateral root development by interfering with polar auxin transport in *Arabidopsis thaliana*. Plant Physiol. Biochem. 139, 738–745. https://doi.org/10.1016/j.plaphy.2019.04.020.

Li, J., Chen, L., Chen, Q., Miao, Y., Peng, Z., Huang, B., Liu, D., Du, H., 2021. Allelopathic effect of *Artemisia argyi* on the germination and growth of various weeds. Sci. Rep. 11, 4303. https://doi.org/10.1038/s41598-021-83752-6.

Li, M., Zhu, Y., Li, S., Zhang, W., Yin, C., Lin, Y., 2022. Regulation of phytohormones on the growth and development of plant root hair. Front. Plant Sci. 13, 865302. https://doi.org/10.3389/fpls.2022.865302.

Lin, Q., Ohashi, Y., Kato, M., Tsuge, T., Gu, H., Qu, L.-J., Aoyama, T., 2015. GLABRA2 directly suppresses basic helix-loop-helix transcription factor genes with diverse functions in root hair development. Plant Cell 27 (10), 2894–2906. https://doi.org/10.1105/tpc.15.00607.

Liu, J., Hasanuzzaman, M., Wen, H., Zhang, J., Peng, T., Sun, H., Zhao, Q., 2019. High temperature and drought stress cause abscisic acid and reactive oxygen species accumulation and suppress seed germination growth in rice. Protoplasma 256 (5), 1217–1227. https://doi.org/10.1007/s00709-019-01354-6.

Lohse, M., Nagel, A., Herter, T., May, P., Schroda, M., Zrenner, R., Tohge, T., Fernie, A.R., Stitt, M., Usadel, B., 2014. Mercator: a fast and simple web server for genome scale functional annotation of plant sequence data. Plant Cell Environ. 37 (5), 1250–1258. https://doi.org/10.1111/pce.12231.

Love, M.I., Huber, W., Anders, S., 2014. Moderated estimation of fold change and dispersion for RNA-seq data with DESeq2. Genome Biol. 15, 550. https://doi.org/10.1186/s13059-014-0550-8.

Lukan, T., Pompe-Novak, M., Baebler, Š., et al., 2020. Precision transcriptomics of viral foci reveals the spatial regulation of immune-signaling genes and identifies RBOHD as an important player in the incompatible interaction between potato virus Y and potato. Plant J. 104, 645–661. https://doi.org/10.1111/tpj.14953.

Lupini, A., Araniti, F., Sunseri, F., Abenavoli, M.R., 2014. Coumarin interacts with auxin polar transport to modify root system architecture in *Arabidopsis thaliana*. Plant Growth Regul. 74 (1), 23–31. https://doi.org/10.1007/s10725-014-9893-0.

Mahdavikia, F., Saharkhiz, M.J., Karami, A., 2017. Defensive response of radish seedlings to the oxidative stress arising from phenolic compounds in the extract of peppermint (*Mentha* × *piperita* L.). Sci. Hortic. 214, 133–140. https://doi.org/10.1016/j.scienta.2016.11.029.

Mincheva, T., Barni, E., Siniscalco, C., 2016. From plant traits to invasion success: impacts of the alien *Fallopia japonica* (Houtt.) Ronse Decraene on two native grassland species. Plant Biosyst. 150 (6), 1348–1357. https://doi.org/10.1080/11263504.2015.1115437.

Mittler, R., Zandalians, S.I., Fichman, Y., Van Breusegem, F., 2022. Reactive oxygen species signalling in plant stress responses. Nat. Rev. Mol. Cell Biol. 23, 663–679. https://doi.org/10.1038/s41580-022-00499-2.

Moravcová, L., Pyšek, P., Jarošik, V., Zákravský, P., 2011. Potential phytotoxic and shading effects of invasive *Fallopia* (Polygonaceae) taxa on the germination of native dominant species. NeoBiota 9, 31–47. https://doi.org/10.3897/neobiota.9.1266.

Murrell, C., Gerber, E., Krebs, C., Parepa, M., Schaffner, U., Bossdorf, O., 2011. Invasive knotweed affects native plants through allelopathy. Am. J. Bot. 98 (1), 38–43. https://doi.org/10.3732/ajb.1000135.

Noctor, G., Reichheld, J.P., Foyer, C.H., 2018. ROS-related redox regulation and signaling in plants. Semin. Cell Develop. Biol. 80, 3–12. https://doi.org/10.1016/j.semcdb.2017.07.013.

Patni, B., Chandra, H., Prakash, M.A., Kumar, G.S., Vitalini, S., Iriti, M., 2018. Rice allelopathy in weed management - an integrated approach. Cell. Mol. Biol. 64 (8), 84–93. https://doi.org/10.14715/cmb/2018.64.8.13.

Renzetti, M., Funck, D., Trovato, M., 2025. Proline and ROS: a unified mechanism in plant development and stress response? Plants 14 (1), 2. https://doi.org/10.3390/plants14010002.

Retzer, K., Weckwerth, W., 2021. The TOR–auxin connection upstream of root hair growth. Plants 10 (1), 150. https://doi.org/10.3390/plants10010150.

Roach, T., Stöggl, W., Baur, T., Kranner, I., 2018. Distress and eustress of reactive electrophiles and relevance to light stress acclimation via stimulation of thiol/disulphide-based redox defences. Free Radic. Biol. Med. 122, 65–73. https://doi.org/10.1016/j.freeradbiomed.2018.03.030.

Robinson, M.D., McCarthy, D.J., Smyth, G.K., 2010. edgeR: a Bioconductor package for differential expression analysis of digital gene expression data. Bioinformatics 26 (1), 139–140. https://doi.org/10.1093/bioinformatics/btp616.

Rossi, F.R., Krapp, A.R., Bisaro, F., Maiale, S.J., Pieckenstain, F.L., Carrillo, N., 2017. Reactive oxygen species generated in chloroplasts contribute to tobacco leaf infection by the necrotrophic fungus *Botrytis cinerea*. Plant J. 92 (5), 761–773. https://doi.org/10.1111/tpj.13718.

Savchenko, T.V., Rolletschek, H., Dehesh, K., 2019. Jasmonates-mediated rewiring of central metabolism regulates adaptive responses. Plant Cell Physiol. 60, 2613–2620. https://doi.org/10.1093/pcp/pcz181.

Schandry, N., Becker, C., 2020. Allelopathic plants: models for studying plant–interkingdom interactions. Trends Plant Sci. 25 (2), 176–185. https://doi.org/10.1016/j.tplants.2019.11.004.

Shirasawa, K., Hirakawa, H., Fukino, N., Kitashiba, H., Isobe, S., 2020. Genome sequence and analysis of a Japanese radish (*Raphanus sativus*) cultivar named 'Sakurajima Daikon' possessing giant root. DNA Res. 27 (2), 1–6. https://doi.org/10.1093/DNARES/DSAA010.

Šoln, K., Žnidaršič, N., Dolenc Koce, J., 2021. Root growth inhibition and ultrastructural changes in radish root tips after treatment with aqueous extracts of *Fallopia japonica* and *F.* × *bohemica* rhizomes. Protoplasma 259, 1111–1124. https://doi.org/10.1007/s00709-021-01668-4.

Šoln, K., Horvat, M., Iskra, J., Dolenc Koce, J., 2022. Inhibitory effects of methanol extracts from *Fallopia japonica* and *F.* × *bohemica* rhizomes and selected phenolic compounds on radish germination and root growth. Chemoecology 32, 159–170. https://doi.org/10.1007/s00049-022-00375-7.

Šoln, K., Žnidaršič, N., Klemenčič, M., Dolenc Koce, J., 2023. *Fallopia japonica* and *Fallopia* × *bohemica* extracts cause ultrastructural and biochemical changes in root tips of radish seedlings. Physiol. Plantarum 175 (5), 14032. https://doi.org/10.1111/ppl.14032.

Song, S.-K., Jeong, D.W., Kim, Y.J., Schiefelbein, J., Lee, M.M., 2024. Negative feedback regulation of GLABRA1 contributes to epidermal cell patterning in the arabidopsis root. Biochem. Biophys. Res. Commun. 737, 150869. https://doi.org/10.1016/j.bbrc.2024.150869.

Strgulc Krajšek, S., Dolenc Koce, J., 2015. Sexual reproduction of knotweed (*Fallopia* sect. *Reynoutria*) in Slovenia. Preslia 87 (1), 17–30.

Sultana, M.H., Alamin, M., Qiu, J., Fan, L., Ye, C., 2023. Transcriptomic profiling reveals candidate allelopathic genes in rice responsible for interactions with barnyardgrass. Front. Plant Sci. 14, 1104951. https://doi.org/10.3389/fpls.2023.1104951.

Tamás, L., Mistrík, I., Zelinová, V., 2017. Heavy metal-induced reactive oxygen species and cell death in barley root tip. Environ. Exp. Bot. 140, 34–40. https://doi.org/10.1016/j.envexpbot.2017.05.016.

Teuschler, L., Gasperl, A., Remele, K., Pfeifhofer, H.W., Müller, M., 2021. Asparagine content is a key factor for acrylamide formation in sweet potato (*Ipomoea batatas* L.) fries. J. Agric. Food Develop. 7, 16–24. https://doi.org/10.30635/2415-0142.2021.07.04.

Tominaga-Wada, R., Kurata, T., Wada, T., 2017. Localization of ENHANCER OF TRY AND CPC1 protein in arabidopsis root epidermis. J. Plant Physiol. 214, 48–52. https://doi.org/10.1016/j.jplph.2017.04.001.

Vissenberg, K., Claeijs, N., Balcerowicz, D., Schoenaers, S., 2020. Hormonal regulation of root hair growth and responses to the environment in arabidopsis. J. Exp. Bot. 71, 2412–2427. https://doi.org/10.1093/jxb/eraa048.

Wickham, H., 2016. ggplot 2: Elegant Graphics for Data Analysis, second ed. Springer.

Yamada, M., Han, X., Benfey, P.N., 2020. RGF1 controls root meristem size through ROS signalling. Nature 577, 85–88. https://doi.org/10.1038/s41586-019-1819-6.

Yan, Z., Wang, D., Cui, H., et al., 2016. Phytotoxicity mechanisms of two coumarin allelochemicals from *Stellera chamaejasme* in lettuce seedlings. Acta Physiol. Plant. 38, 248. https://doi.org/10.1007/s11738-016-2270-z.

Yan, Z., Wang, D., Cui, H., et al., 2018. Effects of artemisinin on root gravitropic response and root system development in *Arabidopsis thaliana*. Plant Growth Regul. 85 (2), 211–220. https://doi.org/10.1007/s10725-018-0384-6.

Yang, J.-C., Zhang, H., Zhang, J.-H., 2012. Root morphology and physiology in relation to the yield formation of rice. J. Integr. Agric. 11, 920–926. https://doi.org/10.1016/S2095-3119(12)60082-3.

Zhang, J., Lin, J.E., Harris, C., Pereira, F.C.M., Wu, F., Blakeslee, J.J., Peer, W.A., 2016. DAO1 catalyzes temporal and tissue-specific oxidative inactivation of auxin in *Arabidopsis thaliana*. Proc. Natl. Acad. Sci. U. S. A 113 (39), 11010–11015. https://doi.org/10.1073/pnas.1604769113.

Zhang, Q., Zheng, X.-Y., Lin, S.-X., Gu, C.-Z., Li, L., Li, J.-Y., Fang, C.-X., He, H.-B., 2019. Transcriptome analysis reveals that barnyard grass exudates increase the allelopathic potential of allelopathic and non-allelopathic rice (Oryza sativa) accessions. Rice 12, 30. https://doi.org/10.1186/s12284-019-0290-1.

Zhang, H., Rutherford, S., Qi, S., Huang, P., Dai, Z., Du, D., 2022. Transcriptome profiling of *Arabidopsis thaliana* roots in response to allelopathic effects of *Conyza canadensis*. Ecotoxicology 31, 53–63. https://doi.org/10.1007/s10646-021-02489-0.

Zhang, L., Chen, K., Li, T., Yuan, S., Li, C., Bai, L., Wang, L., 2023a. Metabolomic and transcriptomic analyses of rice plant interaction with invasive weed *Leptochloa chinensis*. Front. Plant Sci. 14, 1271303. https://doi.org/10.3389/fpls.2023.1271303.

Zhang, Y., Yang, Z., Zhang, Z., Li, Y., Guo, J., Liu, L., Wang, C., Fan, H., Wang, B., Han, G., 2023b. Root hair development and adaptation to abiotic stress. J. Agric. Food Chem. 71, 9573–9598. https://doi.org/10.1021/acs.jafc.2c07741.